ELSEVIER

Contents lists available at ScienceDirect

## **Environment International**

journal homepage: www.elsevier.com/locate/envint





## Correspondence between DOM molecules and microbial community in a subtropical coastal estuary on a spatiotemporal scale

Qi Chen <sup>a,b</sup>, Feng Chen <sup>c</sup>, Michael Gonsior <sup>d</sup>, Yunyun Li <sup>e</sup>, Yu Wang <sup>a,b</sup>, Chen He <sup>e</sup>, Ruanhong Cai <sup>a,b</sup>, Jinxin Xu <sup>a,b</sup>, Yimeng Wang <sup>a,b</sup>, Dapeng Xu <sup>a,b</sup>, Jia Sun <sup>a,b</sup>, Ting Zhang <sup>a,b</sup>, Quan Shi <sup>e</sup>, Nianzhi Jiao <sup>a,b</sup>, Qiang Zheng <sup>a,b,\*</sup>

- <sup>a</sup> State Key Laboratory for Marine Environmental Science, Institute of Marine Microbes and Ecospheres, College of Ocean and Earth Sciences, Xiamen University, Xiang'an Campus, Xiang'an South Road, Xiamen 361102, China
- b Fujian Key Laboratory of Marine Carbon Sequestration, Xiamen University, Xiang'an Campus, Xiang'an South Road, Xiamen 361102, China
- c Institute of Marine and Environmental Technology, University of Maryland Center for Environmental Science, 701 East Pratt Street, Baltimore, MD 21202, United States
- d Chesapeake Biological Laboratory, University of Maryland Center for Environmental Science, 146 Williams Street, Solomons, MD 20688, United States
- e State Key Laboratory of Heavy Oil Processing, China University of Petroleum, 18 Fuxue Road, Changping District, Beijing 102249, China

### ARTICLE INFO

Handling Editor: Da Chen

Keywords: Estuary Microorganism Dissolved organic matter Fluorescent DOM FT-ICR MS

#### ABSTRACT

Dissolved organic matter (DOM) changes in quantity and quality over time and space, especially in highly dynamic coastal estuaries. Bacterioplankton usually display seasonal and spatial variations in abundance and composition in the coastal regions, and influence the DOM pool via assimilation, transformation and release of organic molecules. The change in DOM can also affect the composition of bacterial community. However, little is known on the correspondence between DOM molecules and bacterial composition, particularly through a systematic field survey. In this study, the spatiotemporal signatures of microbial communities and DOM composition in the subtropical coastal estuary of Xiamen are investigated over one and half years. The co-occurrence analysis between bacteria and DOM suggested microorganisms likely transformed the DOM from a relatively high (>400 Da) to a low (<400 Da) molecular weight, corresponding to an apparent increase in overall aromaticity. This might be the reason why microbial transformation renders "dark" organic matter visible in mass spectrometry due to more efficient ionization of microbial metabolites, as well as photodegradation processes. K- and rstrategists exhibited different correlations with two-size categories of DOM molecules owing to their different lifestyles and responses to environmental nutrient conditions. A comparison of the environmental variables and DOM composition with the microbial communities showed that the environmental/DOM variations played a more important role in shaping the microbial communities than vice versa. This study sheds light on the interactions between microbial populations and DOM molecules at the spatiotemporal scale, improving our understanding of microbial roles in marine biogeochemical cycles.

## 1. Introduction

Bacterioplankton and dissolved organic matter (DOM) are two key components in the marine microbial food web, and the transformation of DOM by bacteria can influence biogeochemical cycles in estuaries and oceans (Jiao et al., 2010; Landa et al., 2014; Powers et al., 2018). Bacterioplankton are abundant and diverse in terms of their species composition and metabolic activities in the marine environment (Kujawinski, 2011; Whitman et al., 1998). DOM also contains a mixture

of complex molecules that serve as a major reservoir for the global carbon cycle, amounting to 660 Gt of the carbon in the ocean (Hansell, 2013; Hansell et al., 2012). Bacterioplankton communities are closely associated with the DOM composition because bacterial growth and activity rely on available DOM as an energy substrate (Landa et al., 2014; Zheng et al., 2019). Phytoplankton can produce and release DOM into the ambient environment, most of which is expected to be relatively high molecular weight labile DOM (LDOM) (Azam and Malfatti, 2007; Jiao et al., 2014). These available sources can then be degraded into low

<sup>\*</sup> Corresponding author at: State Key Laboratory for Marine Environmental Science, Institute of Marine Microbes and Ecospheres, College of Ocean and Earth Sciences, Xiamen University, Xiang'an Campus, Xiang'an South Road, Xiamen 361102, China.

E-mail address: zhengqiang@xmu.edu.cn (Q. Zheng).

molecular weight and more recalcitrant DOM (RDOM) by microorganisms (Amon and Benner, 1996; Jiao et al., 2014; Zheng et al., 2019). It has been estimated that approximately half of the carbon fixed by phytoplankton is utilized relatively fast by bacterioplankton and recycled within the microbial food web (Azam and Malfatti 2007; Benner and Amon 2015; Jiao et al., 2010). Therefore, bacterial assimilation, transformation, and respiration of organic matter play an important role in marine carbon cycling (Jiao et al., 2010).

Estuaries are dynamic ecosystems where freshwater mixes with seawater. Riverine flux contributes greatly to the global marine carbon cycle (Bauer and Bianchi, 2011). An estimated annual flux of 0.17-0.36 Gt of dissolved organic carbon (DOC) is transported through rivers into oceans (Dai et al., 2012; Ludwig et al., 1996). During transportation, the molecular composition and structure of riverine DOM are modified through a series of microbial processes (Bauer and Bianchi, 2011), as well as some abiotic processes, such as photodegradation (Mentges et al., 2017; Miranda et al., 2020). Bacteria in coastal estuaries are more abundant and diverse compared to those in open oceans, as estuaries are greatly influenced by rich inorganic nutrients and organic matter input from rivers (Hewson and Fuhrman, 2004; Traving et al., 2017). Significant efforts have been made to investigate the role of bacteria in the DOM cycling in coastal and estuarine environments (Fichot and Benner, 2014; Traving et al., 2017). Many early studies focused on the utilization of DOM by bacteria without considering the complexity of DOM and diversity of bacteria and potential biases created by individual analytical techniques. The "analytical molecular window" obtained by mass spectrometry is critical to understand the FT-ICR MS results, and the ionizable DOM molecules only represent a fraction of total DOM (Patriarca et al., 2020). The high molecular weight and highly reduced "dark" DOM molecules usually contain inefficient ionizable functional groups, and would be invisible in mass spectrometry analyses. Microbial degradation of these "dark" DOM might yield ionizable compounds that could be detected in molecular window of mass spectrometry after significant structural changes resulted from bacterial activity (Vorobev et al., 2018; Zheng et al., 2019).

High-throughput sequencing technology can now generate over a million sequence reads per sample, and this results in thousands of operational taxonomic units (OTUs) or "bacterial populations" (Caporaso et al., 2011; Ibarbalz et al., 2019). Recently, advanced highresolution Fourier transform ion cyclotron resonance mass spectrometry (FT-ICR MS) has been frequently applied to distinguish DOM signatures in complex DOM mixtures in diverse aquatic environments (Gonsior et al., 2017; He et al., 2020a; Koch et al., 2005). Coupling the extensive and diverse data between bacterial composition and DOM molecules it is now feasible using various multivariate statistics, such as the canonical correlation analysis and network analysis (Osterholz et al., 2016; Zhao et al., 2019). A network analysis provides graphical statistics that allow a rapid capture of the potential association between bacterial populations and chemical molecules (Zhao et al., 2019). By analyzing both the DOM molecular and bacterial community compositions along a latitudinal transect in the North Sea, a coupling between active bacterial populations and labile DOM was found, and this interaction was influenced by local phytoplankton blooms and storm mixing (Osterholz et al., 2016) Osterholz et al., (Osterholz et al., 2018) also investigated the composition of DOM molecules and the bacterial community along a salinity gradient in the Delaware Bay during the fall and winter seasons. A higher compositional stability was found in the DOM molecules than the microbial community. Additionally, the bacterial community varied with the changing chemo-diversity of the DOM, which was detected in the viral-lysed picocyanobacteria-derived DOM addition incubations through the means of a network analysis (Zhao et al., 2019). However, we are still at an early stage in understanding the interplay between DOM composition, seasonality, and microbial diversity and activity.

In this study, a subtropical estuary is investigated over 1.5 years with monthly sampling, and a combined analyses of microbial community structures and organic molecular composition is used to describe the

DOM pool and its interplay with microbial communities. High-throughput sequencing is applied to analyze the total and active bacterial communities based on the DNA and RNA sequences of the 16S rRNA gene. The optical analysis and FT-ICR MS are conducted to describe the spatiotemporal signatures of the complex DOM composition. A co-occurrence analysis between OTUs, fluorescence components, organic molecular composition, and environmental variables is performed to distinguish the spatiotemporal distribution patterns of the different bacterial groups and diverse environmental/DOM variables. The ultimate goal is to understand the correspondence between DOM molecules and microbial populations in a subtropical coastal estuary at a spatiotemporal scale.

### 2. Materials and methods

## 2.1. Study area and sample collection

The Jiulong River is the second largest river in Fujian Province, southeast China, and its estuary is located in the western side of Xiamen Island (Fig. S1). The coastal seawater around Xiamen Island is influenced by the Jiulong River freshwater input and by the China Coastal Current, which flows in from the South China Sea (Fig. S1). The estuary-coastal ecosystem has a subtropical monsoon climate with a long, humid summer and a short, dry winter (Yan et al., 2012).

Three sampling sites were monthly investigated in the coastal area surrounding Xiamen Island that represented an ecosystem from the estuary (S03) to the coastal sites (S05 and S07) (~24°N, ~118°E) from December 2017 to July 2019 (except February, August, and November) (Fig. S1). Site S03 is near the base of the Jiulong River catchment, and significantly influenced by river input. Sites S05 and S07 are located at the southern and eastern portion of Xiamen Island respectively. The estuary/coastal ecosystem is predominately semi-diurnal tides, and is a subtropical macrotidal estuary. Considering the sampling not following the same tidal cycle, the estuary site (S03) was greatly influenced by the variations of spring and neap tides which would in part hinder our understanding the spatial pattern. Water samples were collected at approximately 1 m in depth at all the stations. A total of 36 monthly samples were collected from three sites (from the estuarine to coastal water) around Xiamen Island. Water temperature, pH, and salinity were measured using in situ Conductivity-Temperature-Depth (CTD) sensors (Sea-Bird Electronics, Bellevue, WA, USA). All of the seawater samples were pre-filtered through a 20-µm pore size filter to remove eukaryotic organisms and large particles. For bacterial abundance, 2 ml of a sample was mixed with glutaraldehyde (1% v/v) and kept at -80 °C. A one-liter water sample was filtered through a 0.22-µm polycarbonate filter (Millipore, Billerica, MA, USA) and stored at  $-80~^{\circ}\text{C}$  for DNA and RNA extraction. Furthermore, 40 ml of filtrate was transferred to a 50 ml clean tube and stored at  $-20\,^{\circ}\text{C}$  for the nutrient analysis. For the DOM analysis, water samples were filtered through a 0.7-µm GF/F (precombusted at 450 °C for 4 h, Whatman) glass fiber filters. The 20 ml filtered water samples were collected directly into two 40 ml glass vials (acid washed, rinsed with Milli-Q water, and pre-combusted, CNW) and immediately stored at  $-20~^{\circ}\text{C}$  for DOC and fluorescent DOM measurements. One-liter of filtrate was acidified to a pH of 2 in 1L glass bottle (acid washed, rinsed with Milli-Q water, and pre-combusted) for DOM extraction.

## 2.2. Inorganic nutrient and DOM analysis

Inorganic nutrient concentrations including phosphate, nitrate, nitrite, and silicate were measured using the PowerMon Kolorimeter AA3 (Bran  $\,+\,$  Luebbe, Charlotte, NC, USA) followed spectrophotometric methods described in Knap et al., (Knap et al., 1996). The DOC concentrations were measured using a Shimadzu TOC-VCPH analyzer with high-temperature (680 °C) catalytic oxidation. Duplicate samples were defrosted and acidified with phosphoric acid to a pH of 2 before being

analyzed. Potassium hydrogen phthalate standards were used to quantify the DOC.

Fluorescence was determined simultaneously using the Horiba Aqualog system. Samples were scanned from 240 to 600 nm at 5 nm intervals using 1-cm path length quartz cuvettes at room temperature. Excitation (Ex)-emission (Em) matrices (EEMs) were generated at 2.33 nm intervals ranging from 248 to 829 nm at a 2 s integration time. Collected data were analyzed and decomposed into individual fluorescent components using a parallel factor analysis (PARAFAC) as described by Murphy et al., (Murphy et al., 2013) in Matlab 2018 (Fig. S2). All of the samples were normalized by Milli-Q (excitation at 350 nm, emission from 371 to 428 nm).

For the solid phase extracted DOM (SPE-DOM) isolation, one-liter of filtered (0.7-µm GF/F) and acidified (pH 2) seawater was extracted using cartridges (500 mg, Agilent Bond Elut PPL, USA) as described by Dittmar et al., (Dittmaret al., 2008). The molecular composition of SPE-DOM was analyzed using a 9.4 T Bruker Apex Ultra FT-ICR MS with an Apollo II electrospray ion source operated in negative mode (He et al., 2020b). SPE-DOM samples in methanol were injected into the electrospray source at a rate of 250 µL/h and 128 single scans were conducted to acquire each mass spectrum. Data analysis was performed using inhouse software as described in previous study (Zheng et al., 2019). Briefly, a two-mass scale-expanded segment near the most abundant peak of the spectrum was selected, followed by detailed identification of each peak. At least one peak from each class of species was arbitrarily selected as a reference peak. Molecular formulae consisted of up to 100  $^{12}$ C atoms, 2  $^{13}$ C atoms, 200  $^{1}$ H atoms, 4  $^{14}$ N atoms, 20  $^{16}$ O atoms and 2 <sup>32</sup>S atoms.

Individual assigned molecular formula (MF) signal intensities were normalized to the total identified molecular formula intensities with a S/N threshold greater than six (Flerus et al., 2012; Lechtenfeld et al., 2014). The average abundance/value of formulae (CHO, CHON, CHOS, and CHONS), m/z (mass-to-charge ratio), and ratios of hydrogen to carbon (H/C) and oxygen to carbon (O/C) were then calculated for each sample (Flerus et al., 2012). Double bond equivalents (DBE) and modified aromaticity indices (AI $_{\rm mod}$ ) of the identified molecular formulas were calculated as previously described (Koch and Dittmar, 2006).

Double bond equivalents (DBE) =  $C - \frac{1}{2}H + \frac{1}{2}N + 1$ Modified aromatic index (AI<sub>mod</sub>) was calculated as:

$$AI_{mod} = \frac{1 + C - 0.5O - S - 0.5N - 0.5H}{C - 0.5O - S - N}$$

The distribution of identified MFs in all 33 samples was shown in Table S1, and the 1748 common MFs were used to inter-sample rankings analyses as described in Herzsprung et al. (2012, 2017). A rank was assigned to each MF of each sample (Table S1). In order to better visualize the temporal-spatial pattern of DOM molecular composition, four typical samples in two sites (S03 and S07, representing estuary and coastal environments) from Dec. 2017 (winter) and Jul. 2018 (summer) were chosen to draw the van Krevelen diagrams and H/C versus *m/z* diagrams. The inter-sample rankings analysis provided a MF-specific ranking pattern for common MF in all 33 samples. The first rank represents the highest relative intensity of a selected MF among all 33 samples, while the 33nd rank represents that the relative intensity of a component was the lower than that of the other 32 samples (Kamjunke et al., 2017).

## 2.3. Bacterial abundance measurement and the microbial community

The bacterial abundance was determined using bacteria stained with SYBR Green I (Invitrogen, Carlsbad, CA, USA). The cell counts were measured using flow cytometry (BD Accuri C6) based on red versus green fluorescence and side scatter versus green fluorescence plots.

The environmental microbial DNA was extracted using the phenolchloroformisoamyl alcohol method as described by Wang et al., (Wang et al., 2017). RNA extraction was conducted using the zymoBIOMICS DNA/RNA miniprep kit following the manufacturer's instructions. The extracted RNA was then purified and converted to cDNA using the SuperScript Double-Stranded cDNA Synthesis Kit (Invitrogen) according to Wemheuer et al., (Wemheuer et al., 2012). The quality and quantity of DNA and cDNA were measured using a NanoDrop device (Thermo Scientific Inc., Wilmington, DE, USA). Only high-quality samples (A<sub>260/230</sub> > 1.7 and A<sub>260/280</sub> > 1.8) were used for further analysis.

To determine the microbial community structure, the V4-V5 region (forward primers 5'-GTGCCAGCMGCCGCGGTAA-3' and reverse primers 5'-CCGTCAATTCMTTTRAGTTT-3') of the bacterial 16S rRNA gene of the DNA and cDNA samples were amplified using the PCR procedure (Flores et al., 2011). Quantified amplicons were sequenced using the Illumina MiSeq platform (Illumina, San Diego, CA, USA).

## 2.4. Statistical analysis

The heterogeneity of molecular formulas was examined using PCA and PLS-DA. A Spearman's correlation was conducted between four PARAFAC components and identified molecular formulas at a 99% confidence limit, as described by Stubbins et al., (Stubbins et al., 2014), as well as, between the major total and active bacterial OTUs (defined > 0.01%), and environmental variables. The association between the major total and active bacterial OTUs and molecular formulas (MFs) are presented in the co- occurrence network based on a Spearmen's rank correlation coefficient of r > 0.7 (positive network) or r < -0.7(negative network), p < 0.01. The relationships between the environmental variables, DOM composition, and microbial community were determined using a canonical correlation analysis (CCorA) based on an axes of principal coordinate analysis (PCoA) to cover at least a 90% fraction of each dataset (Osterholz et al., 2016). All of the statistical analyses were performed in R 3.6.1 (www.R-project.org), and network visualizations were conducted in Cytoscape V3.7.2.

## 3. Results

## 3.1. Spatiotemporal environmental variables and fluorescent DOM

Located in the subtropical zone, Xiamen has a relatively long summer season (Yan et al., 2012). The four seasons used in this study were defined as spring (March and April), summer (May, June, and July), fall (September and October), and winter (December and January). The environmental variables measured included temperature, salinity, pH, DOC concentration, bacterial abundance, nitrate, nitrite, phosphate, and silicate (Fig. S3). Clear spatial and temporal variations in the environmental variables were found for all of the samples.

The water temperature ranged from 14.8 to 30.0 °C. The average temperature increased from winter and spring (17.4  $\pm$  2.1 °C) and from summer and fall (27.2  $\pm$  2.4 °C). The bacterial abundance and DOC concentration were positively correlated with temperature (Pearson's r=0.68 and 0.48, p<0.01). While the tyrosine-like component, C3, showed a negative correlation with temperature (Pearson's r=-0.66, p<0.01) (Fig. 1A, Fig. S2, Fig. S3).

The salinity ranged from 15.8 to 33.5 in all of the samples. The average salinity increased from the estuary site, S03 (24.1  $\pm$  4.6), to the coastal sites, S05 and S07 (29.6  $\pm$  2.1 and 31.0  $\pm$  1.3, respectively) (Fig. S3B). The inorganic nutrient concentrations, including phosphate, nitrate, nitrite, and silicate, were all negatively correlated with salinity (Pearson's r=-0.77, -0.90, -0.51 and -0.87, p<0.01), suggesting that river-enriched inorganic nutrients were diluted in the coastal area. Fluorescence intensities of humic-like components (C1 and C2) and tryptophan-like C4 component were negatively correlated to salinity (Pearson's r=-0.92, -0.92 and -0.52, p<0.01), signifying riverine inputs of fluorescent DOM to the coastal sites (Fig. 1B, Fig. S2, Fig. S3B). Nitrite was strongly correlated with both temperature (p<0.01, r=0.48) and salinity (p<0.01, r=-0.51). Considering the relatively high

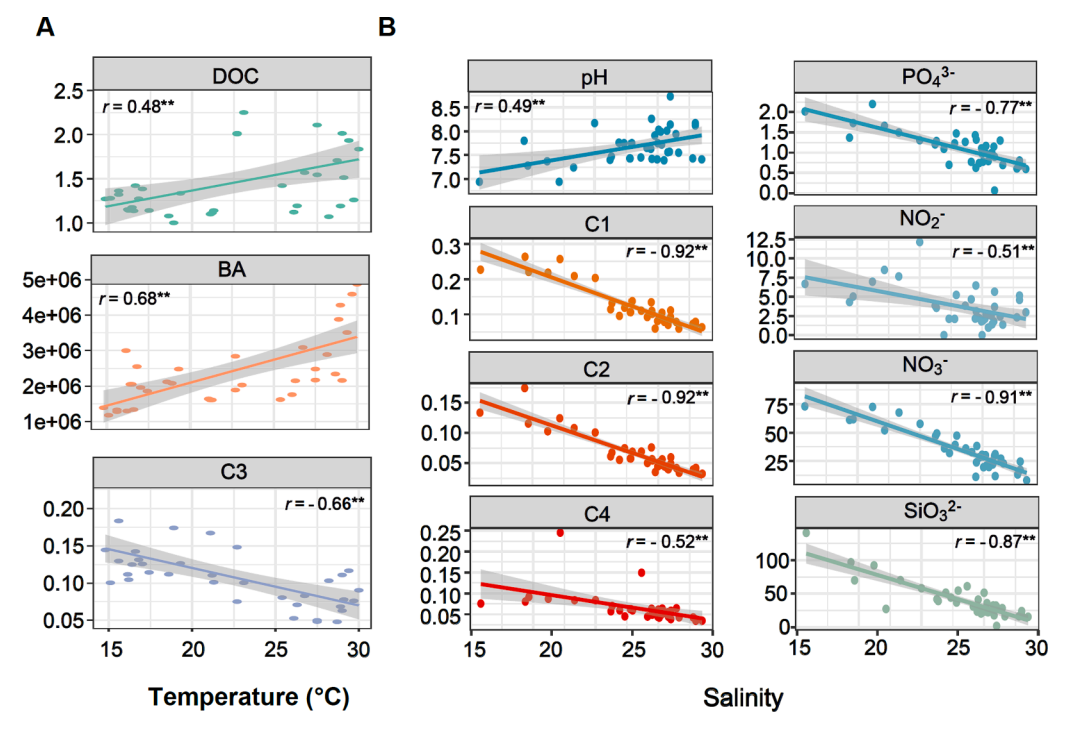


Fig. 1. Spatiotemporal environmental variables and optical properties of the DOM. (A) Temporal-related environmental factors (DOC concentration, bacterial abundance (BA), and fluorophores C3). (B) Spatial-related environmental factors (pH, inorganic nutrients, and fluorophores C1, C2, and C4).

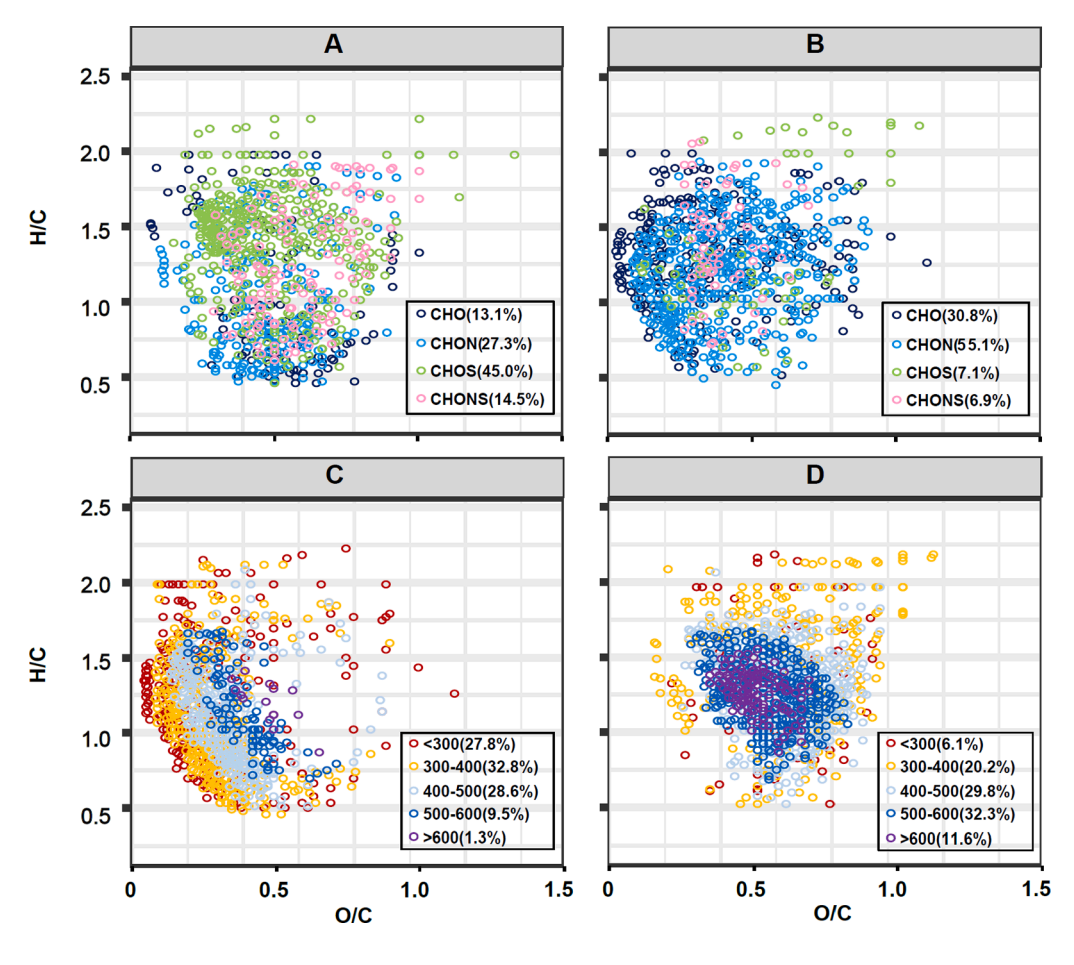


Fig. 2. Molecular characteristics of unique MFs in four different groups including the estuarine group (A), the coastal group (B), the summer group (C), and the fall-winter-spring group (D). These four groups were defined based on the presence and absence of MFs in each category. The different colors represent four major chemical groups in the A and B groups, and the percentage of each chemical group is shown in brackets. The different colors represent five molecular weight ranges in the C and D groups, and percentages of each molecular weight range is also listed in brackets.

 $r^2$  value with salinity, the nitrite was classified into spatial-related variable in the following analyses.

### 3.2. Molecular signature and spatiotemporal distribution of DOM

A total of 8,460 MFs were classified into the CHO, CHON, CHOS, and CHONS groups based on their elemental composition (Fig. S4). The relative intensity of S-containing MFs (including CHOS and CHONS groups) decreased from sites S03, S05, to S07 (14.5  $\pm$  9.5%, 9.2  $\pm$  2.6%, to 8.6  $\pm$  2.5%), while the relative intensity of N-containing MFs (including CHON and CHONS groups) didn't show an obvious variation pattern from sites S03, S05, to S07 (22.1  $\pm$  1.6%, 22.2  $\pm$  0.8%, to 22.3  $\pm$ 0.9%). In addition, the average m/z value was the lowest at site S03 (403.41  $\pm$  9.90), followed by sites S05 and S07 (407.08  $\pm$  9.27 and  $409.02 \pm 11.44$ , respectively). While the average  $AI_{mod}$  value was the highest at site S03 (0.27  $\pm$  0.03), followed by sites S05 and S07 (0.26  $\pm$ 0.04 and 0.24  $\pm$  0.02, respectively). A much lower average m/z but higher AI  $_{mod}$  values (394.14  $\pm$  3.2 and 0.27  $\pm$  0.1, respectively) were present in summer compared to spring (411.91  $\pm$  5.8 and 0.24  $\pm$  0.1, respectively), fall (414.97  $\pm$  11.1 and 0.24  $\pm$  0.1, respectively), and winter (407.81  $\pm$  5.9 and 0.24  $\pm$  0.1, respectively).

A partial least squares discrimination analysis (PLS-DA) and a principal component analysis (PCA) were conducted to sharpen the separation of identified MFs between sites (Fig. S5, Fig. S6). A total of 827, 867, 1,052, and 1,040 molecules were identified as unique MFs for the coastal, estuarine, summer, and fall-winter-spring groups, respectively (Fig. 2, Fig. S7). It should be noticed that the majority of molecules in these four specific DOM pools were only present once in all samples (Table S1). A considerable proportion of the unique S-containing molecules was observed in the estuarine group compared to the coastal group (59.5% versus 14.0%, respectively). A comparison of the unique CHOS molecules in estuary and coastal showed that the relative high molecular weight CHOS molecules (>500 Da) were abundant in coastal group, while the lower molecular weight CHOS molecules (<400 Da) were abundant in the estuary group. The unique N-containing MFs comprised 41.8% and 62.0% of the estuarine and coastal groups, respectively. The O/C ratio and average m/z values were 0.32 and 373.98, respectively, for the summer group, and 0.57 and 473.26, respectively, for the fall-winter-spring group.

The inter-sample rankings analyses were used to understand the differences in DOM-quality between summer and winter, and between estuarine and coastal sites. In order to more easily and transparently

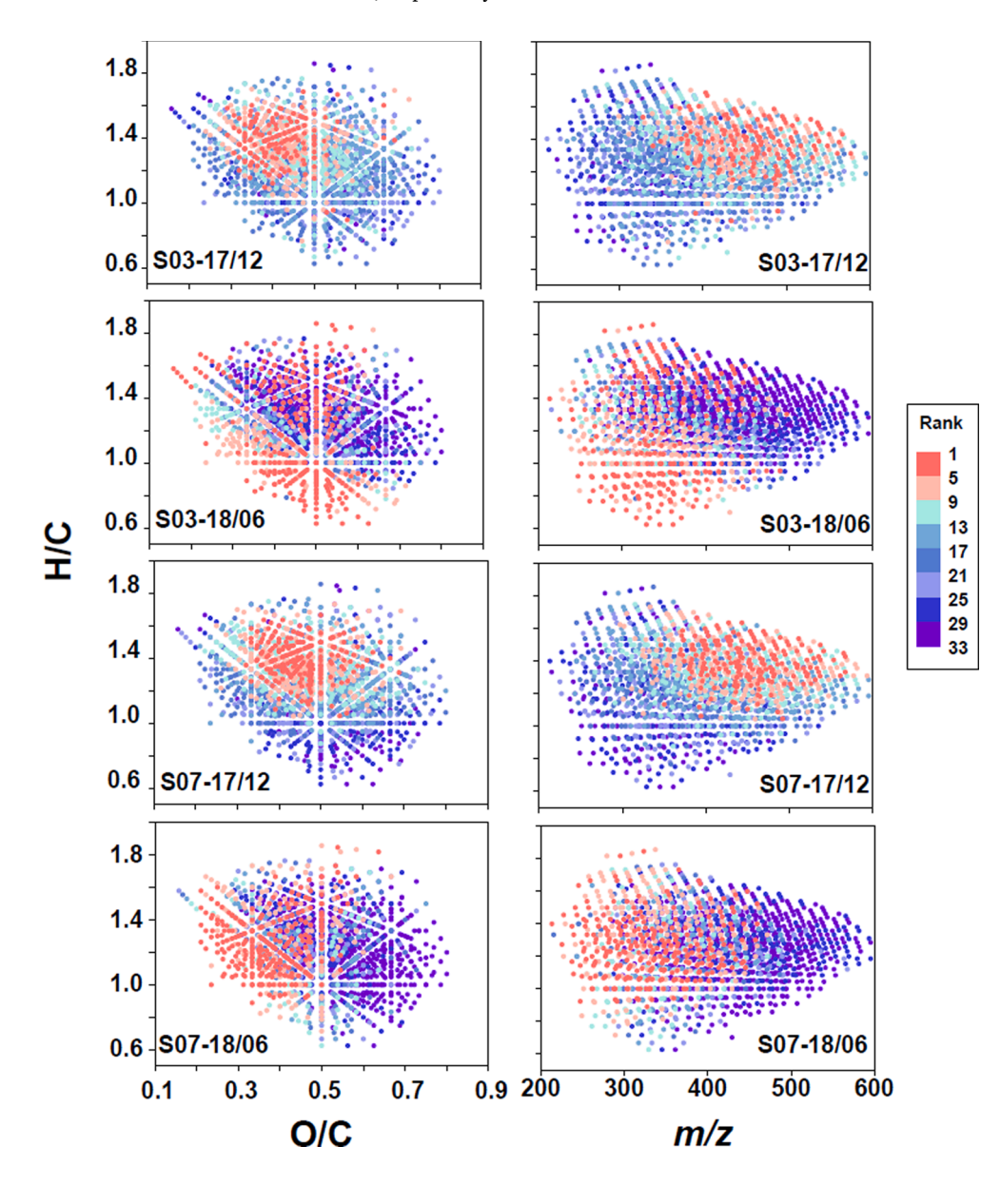


**Fig. 3.** Inter-sample rankings analysis of DOM temporal-spatial characteristics. (left: van Krevelen diagrams, right: H/C versus mass-to-charge (*m*/*z*) diagrams). Four typical samples in two sites (S03 and S07, representing estuary and coastal environments) from Dec. 2017 (17/12, winter) and Jul. 2018 (18/7, summer) were shown in this figure. For visualizing in van Krevelen diagrams, ranks were merged as follows: rank 1-4, rank 5–8, rank 9–12, rank 13–16, rank 17–20, rank 21–24, rank 25–28, rank 29–33, represented by different color bars.

understand the temporal-spatial variations of DOM molecular composition, four typical samples in two sites (S03 and S07, representing estuary and coastal sites) from Dec. 2017 (winter) and Jul. 2018 (summer) were displayed in the van Krevelen diagrams (Fig. 3). Generally, the seasonal DOM quality changes seemed to dominate over the spatial changes. These MFs in the ranks 1-8 (relatively high molecular relative intensities) of two winter samples exhibited relatively high m/z values (most MFs > 400 Da) with H/C > 1.0 and O/C > 0.4, while the MFs in the ranks1-8 of two summer samples displayed lower m/z values (most MFs < 400 Da) with H/C < 1.5 and O/C < 0.5. A comparison between sites S03 and S07 in summer showed that S03 seemed to be more influenced by middle molecular weight highly aromatics (polyphenollikes) from terrestrial origin (H/C < 1.0), and S07 showed ranks 1–4 for lower molecular weight compounds with 1.0 < H/C < 1.5. The DOMquality between sites S03 and S07 in winter didn't display obvious differences which might be caused by the low river flow into the estuary and intensive mixing in the coastal area.

## 3.3. Spatiotemporal features of the microbial community

In this study, bacterial communities were studied based on both DNA and RNA sequences of the 16S rRNA gene. A total of 4,996 and 6,021 OTUs were identified in the DNA and RNA datasets, respectively. For the simplicity, they are referred to as the total and active microbial communities in the following sections. In the total microbial community, the major bacterial groups, Alpha-, Gamma-proteobacteria, and Bacteroidetes comprised 67.7% of total relative abundance. Alphaproteobacteria followed by Cyanobacteria and Gammaproteobacteria contributed a large proportion (64.7%) to the active microbial community (Fig. 4A, Fig. S8A).

To explore the co-occurrence patterns among the total and active microbial communities (at the OTU level), fluorescent DOM (FDOM) components and environmental variables, network analyses were performed (Fig. 4B and Fig. S8B). The DNA-based general network pattern

primarily contained two portions comprised of microbial populations associated with temporal-related and spatial-related environmental variables. In the total microbial community, Actinobacteria, Bacteriodetes, Betaproteobacteria, Deltaproteobacteria, and Marinimicrobia showed higher relative abundances correlating with temperature, DOC concentration, and FDOM C1 component, suggesting that these bacterial groups were sensitive to changes in the temporal-related environmental variables (Fig. 4B). In contrast, Planctomycetes and Verrucomicrobia were more abundant populations that correlated with salinity, inorganic nutrient concentrations, and the FDOM C1, C2, and C4 components, indicating that these bacterial groups were more susceptible to spatialrelated environmental variables. Additionally, the higher relative abundance of Alphaproteobacteria, Cyanobacteria, Gammaproteobacteria, and Thaumarchaeota correlated with most of the variations (environmental variables and FDOM), implying that these bacterial populations were influenced by both spatial and temporal variables. The RNA-based network pattern was similar as the DNA level (Fig. S8B and Supplementary material: Spatiotemporal features of active microbial community).

## 3.4. Linking FDOM components and the DOM molecular signature

It should be noticed that FDOM determines the complex fluorescent DOM, while FT-ICR MS offers an analytical window into the accurate masses of individual molecules. Both samples were obtained using different experimental methods (direct filtered water versus solid-phase extracted material), and they may comprise differences in the molecular composition. Therefore, the similarity in variable behaviors or biological availability was focused on in this study. The number of positive correlations (r > 0.44, p < 0.01) between fluorophores C1-C4 and the MFs were 151, 108, 271, and 123, respectively (Fig. S9). Comparing humic-like fluorophores (C1 and C2) and protein-like fluorophore C3, the MFs that were positively correlated with humic-like fluorophores displayed relatively low average m/z values (330.22 and 321.50 Da,

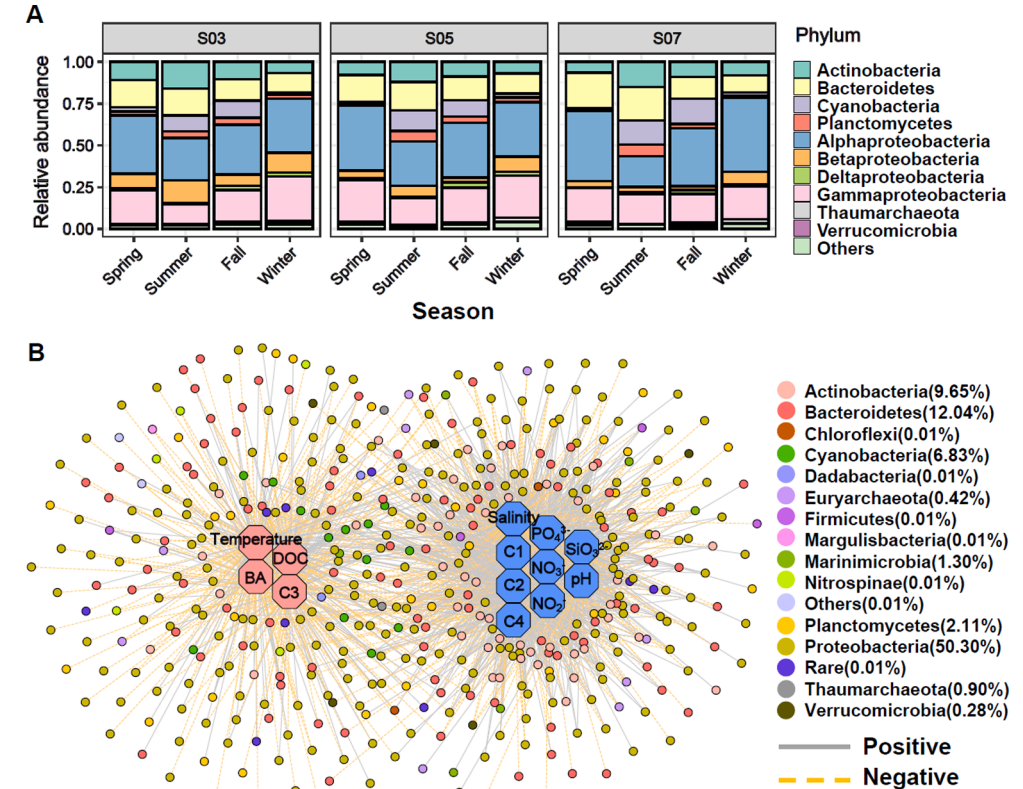


Fig. 4. The total microbial community composition during four seasons and at the three sampling sites (S03, S05, and S07) (A). The network analysis displaying the association of the microbial OTUs with environmental factors and the fluorescent DOM (B). Microbial OTUs (>0.01% relative abundance) based on the DNA sequences of the 16S rRNA gene were analyzed in the network. Correlation patterns were conducted based on the Spearman correlation with statistically significant p values <0.01. Environmental variables and fluorescence components are presented in the octagon nodes, the microbial OTUs those belonging to one phylum are shown in the same color circle and percentages of each phylum is also listed in brackets. The solid and dash lines represent the positive and negative correlations, respectively.

respectively), but relatively high  $AI_{mod}$  values (0.34 and 0.30, respectively). While the protein-like fluorophore C3 was positively correlated with the MFs those had higher average m/z (510.34 Da) and lower  $AI_{mod}$  (0.18) values. However, the molecules that were positively correlated with protein-like fluorophore C4 exhibited no clear pattern due to the non-conservative behavior of C4. The fluorophore of tryptophan-like C4 was reported to decrease from the upstream (fresh water) of the Jiulong River and estuary to the coastal water in the previous study, exhibiting in part terrestrial source properties (Guo et al., 2011). However, C4 component also received widespread additions (likely from autochthonous production) in the estuary, suggesting that it may come from multiple sources (Guo et al., 2011).

## 3.5. Co-occurrence network between the microbial community and DOM $\it molecules$

The correlations between the OTUs from the total microbial composition and the identified MFs were computed to evaluate the relationship between microbial populations and DOM molecules (Fig. 5). Overall, the average m/z and  $AI_{mod}$  of the MFs that participated in the positive network were 390.82 Da and 0.29, respectively. However, much higher average m/z (427.47 Da) but lower  $AI_{mod}$  (0.24) values were detected in the negative networks.

Four major subnetworks (two positive subnetworks, DPM1 and DPM2; two negative subnetworks, DNM1 and DNM2), which contained 231 OTUs and 1,416 MFs, accounted for a considerable relative

abundance/intensity of the total microbial community (45%) and the total identified molecules (45%) (Fig. 5). In addition, the MFs in the subnetwork DPM1 displayed low average m/z (323.83 Da) and high  $AI_{mod}$  (0.34) values, while the MFs in DPM2 exhibited high average m/z (497.52 Da) and low  $AI_{mod}$  (0.20) values. In these two complex negative subnetworks, the average m/z values for DNM1 and DNM2 were 497.83 Da and 305.38 Da, respectively, and the corresponding  $AI_{mod}$  values were 0.18 and 0.35, respectively.

Particularly, 112 common OTUs were found in both the positive DPM1 and negative DNM1 subnetworks, suggesting these bacterial populations were positively correlated with low m/z (322.53 Da) and high  $AI_{mod}$  (0.35) MFs. In addition, they were negatively correlated with high m/z (497.64 Da) and low AI $_{mod}$  (0.18) MFs. These OTUs comprised 10% of the total community and significantly correlated with 41% (relative intensity) of molecules (Partial Mantel test r = 0.52, p < 0.001). A majority of these taxa were Alphaproteobateria, especially Rhodobacteraceae, followed by Actinobacteria and Betaproteobacteria (mostly Rhodocyclaceae). In contrast, there were 31 mutual OTUs in DPM2 and DNM2, and those microorganisms were positively correlated with high  $\ensuremath{\textit{m/z}}$  (497.87 Da) and low  $\ensuremath{\text{AI}_{\text{mod}}}$  (0.18) MFs and negatively correlated with low m/z (304.43 Da) and high  $AI_{mod}$  (0.35) MFs. These 31 OTUs made up 22% of the relative abundance of the total community and were significantly correlated with 30% of the total molecular relative intensity (Partial Mantel test r = 0.50, p < 0.001). The dominant taxa were Alphaproteobateria, primarily SAR11, Gammaproteobateria, and Betaproteobacteria (mostly Methylophilaceae). The co-occurrence networks

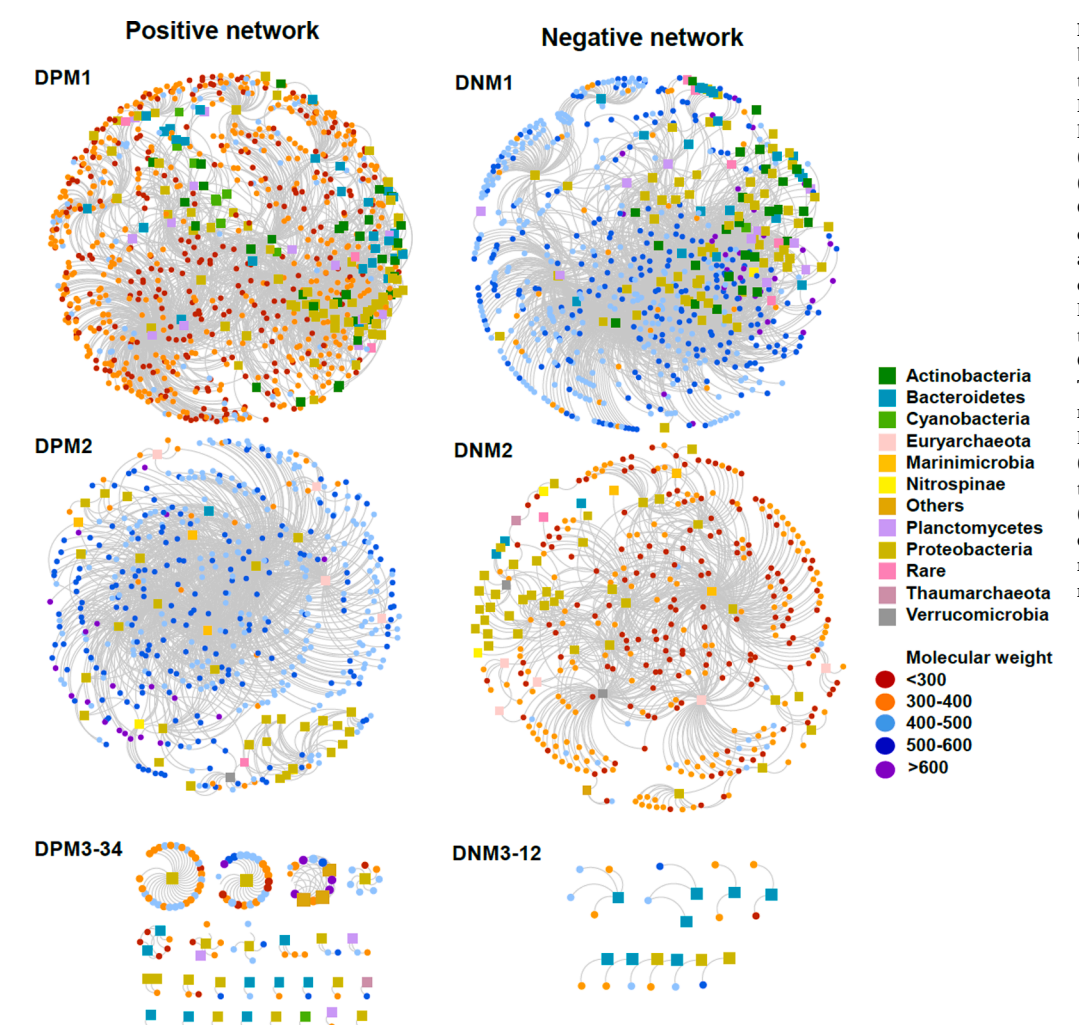


Fig. 5. The co-occurrence network based on the Spearman correlation between the total microbial OTUs and DOM molecules. Spearmen's rank correlation coefficient is strong at r > 0.7(Positive network, upper) and r < -0.7(Negative network, lower), p < 0.01. The OTUs with a > 0.01% relative abundance were included in the network analysis. The positive networks consisted of 1,533 nodes (229 OTUs and 1,304 MFs) and 4,361 edges, while the negative networks included 1,075 nodes (193 OTUs and 882 MFs) and 3,993 edges. The positive networks comprised two major complex subnetworks (DPM1 and DPM2) and 32 simple components (DPM3-34). The negative networks contained two major complex subnetworks (DNM1 and DNM2) and ten simple components (DNM3-12). The colors represent the microbial taxonomy and molecular weight ranges.

between RNA-based OTUs and organic molecules also had similar patterns as the DNA/MFs (Fig. S10 and Supplementary material: Cooccurrence network between active microbial community and DOM molecules).

The degree indicating the connections between the MFs and OTUs was calculated. The average degree number of MFs was five. The correlated MFs were then classified into "keystone" (degree > 10) and "independent" (degree = 1) DOM groups (Fig. S11). The "keystone" DOM molecules represented key intermediate substrates or products that interacted with multiple microbial populations consisting of either higher (506.36 Da, n = 47) or lower (372.79 Da, n = 119) molecular weight molecules in negative and positive networks, respectively. However, the "independent" DOM group represented these unique molecules that were only associated with one specific microbial population comprised of a more diverse and wider size range of molecules. The average degree number of OTUs was 31. Similarly, OTUs with high connectivity (degree > 60) were classified as "generalists," which can potentially utilize or produce multiple DOM molecules. The majority (75%) of these taxa were Alphaproteobateria. OTUs with low connectivity (degree = 1) were defined as "specialists", which prefer specific molecules. The most dominant taxa (35%) was Bacteroidetes.

# 3.6. Linking environmental variables, diverse DOM compositions, and the microbial community

Because the relationship between microorganisms and DOM is bidirectional, bacteria can consume or produce DOM molecules. In addition, the labile DOM composition can shape the microbial community. Therefore, the bimultivariate redundancy coefficients were calculated to evaluate one dataset as explained by another dataset (and vice versa) (Table 1). Generally, the coefficients between the environmental/DOM variations and the total community (Env|DNA 0.87|0.16; FDOM|DNA 0.79|0.14; and MFs|DNA 0.62|0.40) were higher than vice versa. The results were similar in the RNA-based active community, and the coefficients between environmental/DOM variations and active community (Env|RNA 0.89|0.16; FDOM|RNA 0.81|0.15; and MFs|RNA 0.60|0.38) were higher than vice versa. These results indicated that abiotic variables had more impact on the biotic composition. In addition, environmental variables (0.87 and 0.89) and FDOM (0.79 and 0.81) presented a higher proportion of both the total and active microbial compositions than the MFs (0.62 and 0.60), suggesting that the environmental variables and FDOM were better correlated with the (total and active) microbial community compared to the MFs. Also, comparatively lower coefficients were found between the RNA-based association with the MFs (0.60|0.38) than the DNA-based association with the MFs (0.62|0.40).

Table 1
Redundancy coefficients derived from the canonical correlation analysis (CCorA) based on microbial OTUs (DNA or RNA), environmental variables (env), fluorescence components (FDOM), and identified organic molecules (MFs).

	Redundancy coefficients
MFs on DNA/DNA on MFs	0.62/0.40
FDOM on DNA/DNA on FDOM	0.79/0.14
Env on DNA/DNA on Env	0.87/0.16
MFs on RNA/RNA on MFs	0.60/0.38
FDOM on RNA/RNA on FDOM	0.81/0.15
Env on RNA/RNA on Env	0.89/0.16
DNA on RNA/RNA on DNA	0.77/0.77
MFs on FDOM/FDOM on MFs	0.13/0.47
Env on MFs/MFs on env	0.47/0.13
Env on FDOM/FDOM on env	0.50/0.50

Bimultivariate redundancy coefficients for one dataset as explained by another dataset (and vice versa).

### 4. Discussion

This study linked the microbial community with environmental variables and FDOM, as well as DOM molecular composition, and analyzed the spatiotemporal distribution patterns of bacterial groups. The dynamics of the total and active bacterial groups were able to be distinguished over the seasons in a coastal estuary. In addition, correlation analyses between microbial communities and DOM molecules indicated that different bacterial groups were negatively and positively correlated with different sizes of molecules (>400 Da or < 400 Da), respectively. These findings deepened the understanding of microbial processing DOM in coastal carbon cycling.

### 4.1. Spatiotemporal variation in the DOM composition

Allochthonous and autochthonous organic matters together contributed to the estuarine-coastal DOM pool. S-containing organic molecules were more abundant and unique in the estuary, while diverse and distinctive N-containing molecules accumulated in the coastal area (Fig. 2). The S-containing molecules could be derived from autochthonous production, as well as a great contribution from anthropogenic activities (Flerus et al., 2012; Ksjonzek et al., 2016). A higher portion of S-containing organic matter has been reported in effluent compositions and in an estuary affected by sewage (Gonsior et al., 2011; He et al., 2020b). Hydrodesulphurization in sediments and resuspension of these material may also lead to abundant S-containing DOM signatures in estuarine regions (Schmidt et al., 2009; Gomez-Saez et al., 2017; Pohlabeln et al., 2017). The enriched unique N-containing molecules in the coastal area could be derived from phytoplankton primary production and heterotrophic bacterial secondary metabolism, as well as photochemical degradation with potential preference for CHO group molecules (Blough 2002; Seidel et al., 2016; Seidel et al., 2015).

The fact that the DOC concentration was relatively high in summer and fall compared to spring and winter could be related to high primary production caused by seasonal phytoplankton growth/bloom, river inputs, or strong water column mixing caused by storms (Fig. 6) (Wang et al., 2019; Yang et al., 2015). Typically, there exists successions of diatoms and Synechococcus with high abundances in the studied region (Yang et al., 2012; Wang et al., 2019; Chen et al., 2021). Both diatomand Synechococcus-derived DOM consist of labile tyrosine-like fluorophore with a relatively high fluorescence intensity that can be utilized by bacteria to produce more humic-like fluorescent components (Romera-Castillo et al., 2011; Lønborg et al., 2013; Zheng et al., 2019). In the present study, the labile tyrosine-like fluorophore C3 was almost depleted in summer (Fig. 1A, Fig. S3A), while two relatively recalcitrant humic-like components, C1 and C2, were the highest in summer (Fig. 1A, Fig. S3A) and could be caused by microbial transformation (Romera-Castillo et al., 2011; Zheng et al., 2019). In addition, the average AI<sub>mod</sub> value of the MFs which partly reflects the molecular recalcitrant level was the highest, but the average m/z value was the lowest in summer (Fig. S4). Decreased m/z and increased  $AI_{mod}$  values were also detected in the transformation of Synechococcus-derived DOM by environmental microorganisms (Zheng et al., 2019). It is therefore likely that the environmental microbial processing of DOM might have contributed to the production and accumulation of humic-like components (as revealed by the FDOM results) and lower molecular weight molecules (as revealed by the FT-ICR MS results), especially in the summer.

## 4.2. Microbial mediated DOM molecular transformation

It should be noted that bacterial degradation of high molecular weight and highly reduced "dark" DOM might yield ionizable compounds that would not be visible in mass spectrometry prior to significant structural changes associated with this microbial degradation. Unfortunately, direct infusion ultrahigh resolution mass spectrometry is

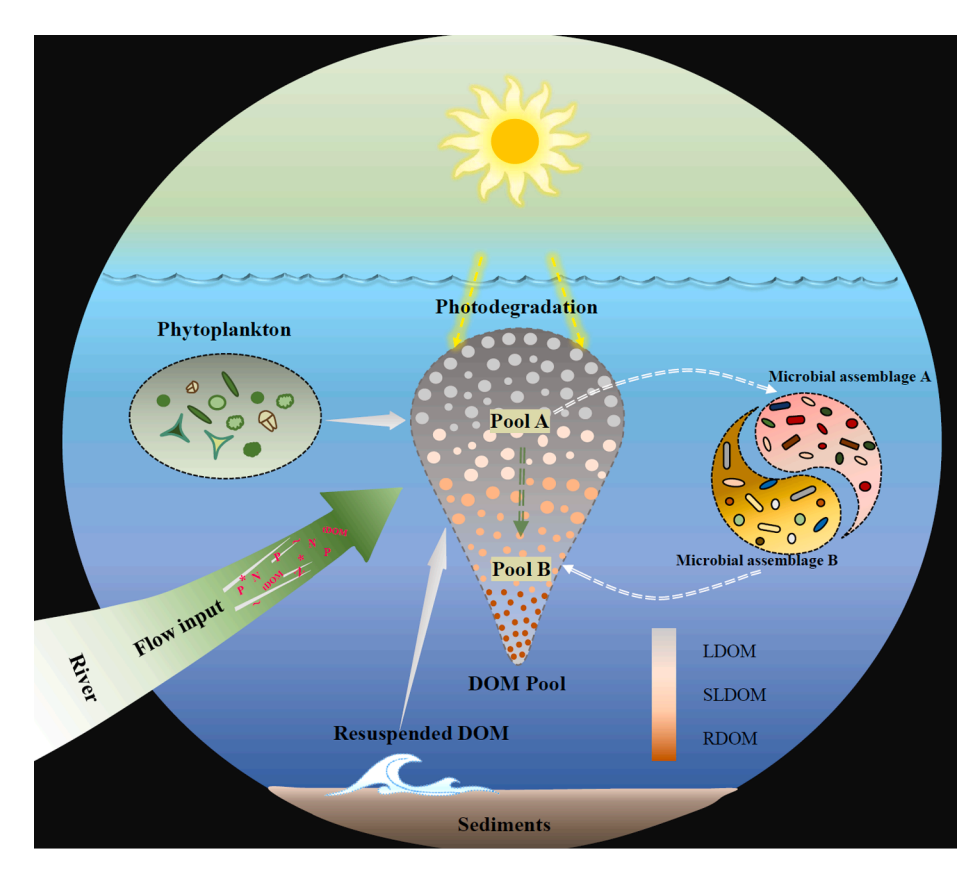


Fig. 6. Schematic of the coastal microorganismmediated dissolved organic matter transformation. The coastal DOM is a mixed pool of organic matter driven by riverine input, phytoplankton primary production, sediment resuspension, and intensive anthropogenic disturbance (e.g., sewage discharge and aquaculture). During transportation, organic molecular composition, structure, and bioavailability are modified through a series of microbial metabolic processes, as well as some abiotic processes, such as photodegradation. Microbial metabolic activities likely transform relatively high molecular weight and labile DOM (Pool A) into relatively low molecular weight and recalcitrant DOM (Pool B). During microbial degradation of DOM, microbial assemblages A and B, corresponding to r- and K-strategists, respectively, display different correlations with different biological availabilities of DOM (Pools A and B). LDOM, labile DOM, SLDOM, semi-labile DOM, RDOM, recalcitrant DOM. Pool A, relatively high molecular weight and labile DOM; Pool B, relatively low molecular weight and recalcitrant DOM. Microbial assemblage A, r-strategists; Microbial assemblage B, Kstrategists.

prone to favor highly ionizable compounds and may severely suppress high molecular weight reduced molecules that contain difficult to ionize functional groups. In present study, it is likely that the environmental microorganisms efficiently transformed high molecular weight and highly reduced "dark" DOM into relatively small and ionizable compounds that could be captured by the "analytical window" of FT-ICR MS in the estuary-coastal ecosystem, especially in summer.

The FT-ICR MS provided a window for the identification of lowmolecular-weight (LMW) DOM (200-800 Da). Correspondence between the molecular size and the microbial community was established when the molecular size (>400 Da or < 400 Da) was positively or negatively correlated with different microbial groups (Fig. 5). However, these correlations did not necessarily allow a resolution to the transformation between the microbial community and the DOM composition (Osterholzet al., 2016). Rather, that generated directions for further detailed investigations of microbial degradation and production of DOM. Our previous incubation experiments supported that microbial communities tended to uptake high molecular weight DOM (>400 Da) and produce low molecular weights (<400 Da) with increasing aromaticity (Zheng et al., 2019). Microbial newly formed DOM molecules were between 280 and 320 Da in a phytoplankton bloom incubation (Osterholz et al., 2015) and < 400 Da in a riverine DOM degradation experiment (Kamjunke et al., 2017). Additionally, the utilization of labile protein-like FDOM components (e.g., C3 positively correlated with > 400 Da molecules) has been typically accompanied by the accumulation of relatively recalcitrant aromatic/humic-like compounds (e.g., both C1 and C2 positive correlated with < 400 Da molecules) in incubation experiments (Amaral et al., 2016; Zheng et al., 2019). Molecules with higher m/z values (>400 Da) but lower AI<sub>mod</sub> were found in the negative network, while molecules with lower m/z values (<400 Da) and higher AImod were found in the positive network based on the DNA dataset (Fig. 5). These results also imply that the microbes likely transformed from high (>400 Da) to low molecular weight (<400 Da) DOM molecules, corresponding to increasing aromaticity in the coastal estuary.

Examples of such microbial enzymatic activity-mediated transformations are demethoxylation (remove  $CH_2O$ ), deacetylation ( $C_2H_2O_2$ ), and decarboxylation ( $CO_2$ ) (Vorobev et al., 2018), and all of these processes make transformed molecules with much lower m/z and O/C values, especially in summer when there is the highest microbial activity in our studied regions. These processes have been proven to be three of the most frequent potential microbial mediated transformations in elemental composition in coastal seawater incubations (Vorobev et al., 2018). In addition, acetate has been identified as one of the most important photochemical products in marine surface waters, suggesting photodegradation also contributes to organic molecular decarboxylation processes (Sheik et al., 2020; Wetze et al., 1995).

According to microbial lifestyle strategies, marine heterotrophic bacteria can be classified into two ecological categories, r- and K-strategists (Giovannoni, 2017; Luo et al., 2013). K-strategists (e.g., SAR11) usually contain streamlined genomes and have high substrate affinity and low growth rates (Giovannoni, 2017; Luo et al., 2013). These bacterial populations are commonly abundant in the environment and exhibit obvious growth advantages under extremely low substrate concentrations. However, the other group, r-strategists (e.g., Rhodobacteraceae) have versatile metabolic capabilities and can rapidly respond to rich organic matter conditions with high growth rates (Luo et al., 2013). Thus, the 112 OTUs (primarily Rhodobacteraceae) that comprised 10% of the total community could be roughly classified as r-strategists, and 31 OTUs (especially SAR11) consisting of 22% of the total community were K-strategists. Generally, these 112 OTUs will respond to nutrient enrichment, especially to high concentrations of labile DOM based on their r-strategist's ecological strategies. These bacterial populations usually display high growth rates corresponding to the consumption and utilization of DOM, and result in high relative abundances. However, these 31 OTUs will decrease their relative abundance as result of the slow growth under the same surroundings based on their K-strategist's ecological strategies, despite a potential increase in their absolute numbers. The different microbial lifestyles and responses to nutrient conditions may be accounted for their different correlations with DOM molecules

Q. Chen et al.

The molecular composition that was considered to be the "keystone" DOM group (connected with over 10 OTUs) were higher or lower molecular weights corresponding to different molecular size ranges in the negative and positive networks (Fig. S11). These two molecular sizes of DOM were general substrates or products correlated to abundant microorganisms and potentially had higher turnover or production rates by microbial communities. High molecular weight molecules that are negatively correlated with microbes usually decrease their relative intensities through microbial transformation (Vorobev et al., 2018; Zheng et al., 2019). In contrast, the "independent" DOM groups (connected with 1 OTU) consisted of a wider range of molecular compositions on the molecular mass level or atom ratios. This means that some specific microbial populations might uptake or release unique DOM molecules, which greatly increases the complexity of the microbial community and environmental DOM (Tanentzap et al., 2019).

The major microorganisms in the "generalists" group were Alphaproteobateria (e.g., Rhodobacteraceae). Members in this group are considered to be generalist in their response to extracellular polymeric substances of phytoplankton blooms (Teeling et al., 2012). Alphaproteobateria have also been found to be associated with diverse molecules derived from the virus-lysed Synechococcus (Zhao et al., 2019). Members of Bacteroidetes (e.g., Flavobacteria) have been widely classified as "specialists" as result of their capacity to degrade specific highmolecular-weight (HMW, > 1,000 Da) DOM molecules (Zhao et al., 2019; Zheng et al., 2018). However, these HMW DOM have not been observed in the FT-ICR MS, possibly due to their suspected much higher suppression and presumably weak ionization efficiencies, which also partially accounts for the low connections between Bacteroidetes and the LMW DOM molecules. Generalists and specialists display different organic matter utilization capacities and respond to different phases of phytoplankton blooms (Teeling et al., 2012).

The network analyses comprised  $\sim 50\%$  of the total microbial community and the total identified molecules, respectively. Here it should be noted that most microorganisms could be detected by high throughput sequencing, however, only a fraction of DOM molecules could be characterized as result of the PPL extraction efficiency ( $\sim 40-50\%$  in this study), unknown ionizable efficiency in ESI negative mode and so on. That may account for only half of microbial community in the networks, and the other microorganisms might utilize some "dark" DOM molecules or particulate organic matter those couldn't be captured by FT-ICR MS. The environmental DOM pool comprised a considerable amount of recalcitrant and stable molecules those might not be involved in further microbial transformation (Jiao et al., 2010), and these recalcitrant DOM would be absent in the interactive networks.

# 4.3. Interactions between the environmental variables, DOM composition, and the microbial community

Generally, the correlation between DNA and MFs was stronger than that based on the RNA and MFs (Table 1). Active microbial groups that are usually associated with labile larger molecular weight compounds or smaller monomers, and these are discriminated against by the SPE-DOM isolation that captured more semi-labile and recalcitrant molecules with much longer turnover times (Osterholz et al., 2016; Tanentzap et al., 2019). The FDOM accounted for a portion of the optical properties of the DOM and efficiently reflected DOM utilization and production (Fox et al., 2017; Stedmon et al., 2011). The correlation between RNA and FDOM components was slightly stronger than the DNA and the FDOM, indicating that FDOM might be closely associated with in situ microbial community activities. Additionally, the bi-multivariate redundancy coefficients analyses revealed that the environmental DOM composition (MFs and FDOM) affected the microbial community structure (DNA and RNA) stronger than vice versa. This result supported that the effect of DOM on the microbial community structure was stronger than the effect of microbes on the DOM (Tanentzap et al., 2019). Increased DOM input provided more diverse and available DOM sources, which resulted in more niches for different microbial communities (Tanentzap et al., 2019). In addition, the environmental variables and DOM chemical composition showed a higher correlation to the total and active microbial community than vice versa, suggesting that environmental selection played a more important role in shaping the microbial community than microbial process contributing to the environmental variations. In particular, the interaction between microbes and some environmental variables (e.g., salinity and temperature) was one directional. For example, salinity can select for certain microorganisms due to their salt tolerance (Osterholz et al., 2018), while these microorganisms have no impact on the ambient salinity.

Riverine input and intensive anthropogenic activities (e.g., sewage discharge and aquaculture) bring a considerable amount of terrestrial/ allochthonous DOM and inorganic nutrients to the estuary-coastal ecosystem (Bauer and Bianchi, 2011; Dai et al., 2012) (Fig. 6). The coastal eutrophication, as well as global warming, stimulate the frequent phytoplankton blooms in the coastal area, which contribute large amounts of autochthonous labile DOM to the coastal region (Lønborg et al., 2020). Bacterioplankton respond quickly to DOM released via riverine runoff and phytoplankton blooms, and can reduce dissolved oxygen in the water due to increased microbial respiration (Bograd et al., 2008; Diaz et al., 2019). The consequent environmental effects (e. g., hypoxia and acidification) will have a significant impact on environmental and human health (via polluted or toxin-containing seafood) (Watson et al., 2017; Krogh et al., 2018). In this study, we investigated the molecular interaction between environmental DOM and microorganisms, and provided a new insight to microbial processing of the coastal DOM pool under variable environmental conditions.

### 5. Conclusions

The time series sampling in the estuarine-coastal region could be thought as a long- term mesocosm incubation system (Fig. 6). Microorganisms take significant parts in utilization and transformation of allochthonous and autochthonous organic matter. The strong estuarine gradients (e.g., salinity and inorganic nutrients) and seasonal variations shaped a high degree of the microbial diversity and caused considerable spatial and temporal variability. This study demonstrated the spatiotemporal features of the diverse DOM composition and microbial community signatures and their interplay in an estuary-coastal ecosystem. Estuarine input contributed humic-like FDOM, as well as the S-containing organic molecules, to the coastal ecosystem. The DOM molecules with the lowest average m/z and O/C values were detected during summer. The variations of fluorescent DOM components and DOM molecular composition, in part reflect the contribution of allochthonous and autochthonous organic matter to the in situ DOM pool. The distribution of the total and active microbial groups was clearly associated with temporal-, spatial-, or spatiotemporal-related environmental variables. Diverse microbial groups were correlated with different sizes and categories of organic molecules, emphasizing the positive connections between chemo-diversity and biodiversity in the estuary. Microorganisms tended to transform from relatively high (>400 Da) to low (<400 Da) molecular weight molecules corresponding to increasing aromaticity, which was likely a response to make "dark" DOM visible through the mass spectrometric analytical window by increasing the ionization efficiencies upon microbial degradation of presumably reduced high molecular weight DOM. Environmental/DOM variations played a more important role in shaping the microbial communities than vice versa. The correlation between RNA and the FDOM components was stronger than that based on DNA|FDOM, DNA|MFs or RNA|MFs, indicating that the FDOM was closely associated with in situ microbial community activities. It is also essential to further identify the relationship between specific microorganisms and organic compounds, as well as the physiological or ecological effect of molecular sizes.

### CRediT authorship contribution statement

Qi Chen: Methodology, Writing - original draft, Formal analysis, Visualization. Feng Chen: Supervision, Writing - review & editing. Michael Gonsior: Methodology, Writing - review & editing. Yunyun Li: Methodology, Software, Data curation. Yu Wang: Data curation, Visualization, Investigation, Writing - review & editing. Chen He: Data curation, Software, Investigation. Ruanhong Cai: Data curation, Writing - review & editing. Jinxin Xu: Data curation, Writing - review & editing. Yimeng Wang: Visualization, Investigation. Dapeng Xu: Writing - review & editing. Jia Sun: Data curation, Visualization, Investigation. Ting Zhang: Visualization, Investigation. Quan Shi: Methodology, Software, Investigation. Nianzhi Jiao: Writing - review & editing. Qiang Zheng: Supervision, Conceptualization, Formal analysis, Investigation, Writing - review & editing.

### **Declaration of Competing Interest**

The authors declare that they have no known competing financial interests or personal relationships that could have appeared to influence the work reported in this paper.

### Acknowledgements

This work was supported by the National Key Research Programs (2018YFA0605800), the Senior User Project of RV KEXUE (KEX-UE2019GZ03), the National Natural Science Foundation of China (41776145, 41876150, 91751207 and 41861144018), the Fundamental Research Funds for the Central Universities (20720190095), and the Project of Environmental Protection Science and Technology of Fujian Province of China (2021R005).

## Author contributions

QZ, NJ and FC conceived and designed the experiments. QC, QZ, YYL, RC, CH and QS conducted the experiments. QC, YW, YYL, FC, RC, MG, CH, YMW, DX, TZ and QS analyzed the data. All of the authors assisted in writing the manuscript, discussed the results, and commented on the manuscript.

## Data availability

Sequence data were deposited in the National Center for Biotechnology Information (NCBI) Sequence Read Archive with BioProject PRJNA661148 (DNA data) and PRJNA661155 (RNA data). FT-ICR MS data were deposited on figshare with doi: 10.6084/m9.figshare.12911192.v1.

## Appendix A. Supplementary material

Supplementary data to this article can be found online at https://doi. org/10.1016/j.envint.2021.106558.

## References

- Amaral, V., Graeber, D., Calliari, D., Alonso, C., 2016. Strong linkages between DOM optical properties and main clades of aquatic bacteria. Limnol. Oceanogr. 61, 906–918. https://doi.org/10.1002/lpo.10258.
- Amon, R.M.W., Benner, R., 1996. Bacterial utilization of different size classes of dissolved organic matter. Limnol. Oceanogr. 41, 41–51. https://doi.org/10.4319/
- Azam, F., Malfatti, F., 2007. Microbial structuring of marine ecosystems. Nat. Rev. Microbiol. 5, 782–791. https://doi.org/10.1038/nrmicro1747.
- Bauer, J., Bianchi, T., 2011. 5.02—dissolved organic carbon cycling and transformation. Treatise on Estuarine Coastal Science 5, 7–67. https://doi.org/10.1016/B978-0-12-374711-2.00502-7.
- Benner, R., Amon, R.M., 2015. The size-reactivity continuum of major bioelements in the ocean. Ann. Rev. Mar. Sci. 7, 185–205. https://doi.org/10.1146/annurev-marine-010213-135126.

- Blough, N.V., 2002. Chromophoric DOM in the coastal environment. Biogeochem.

  Marine Dissolved Organic Matter 509–546. https://doi.org/10.1016/B978-01233841-2/50012-9
- Bograd, S.J., Castro, C.G., Di Lorenzo, E., Palacios, D.M., Bailey, H., Gilly, W., Chavez, F. P., 2008. Oxygen declines and the shoaling of the hypoxic boundary in the California Current. Geophys. Res. Lett. 35 https://doi.org/10.1029/2008gl034185.
- Caporaso, J.G., Lauber, C.L., Walters, W.A., Berg-Lyons, D., Lozupone, C.A., Turnbaugh, P.J., Fierer, N., Knight, R., 2011. Global patterns of 16S rRNA diversity at a depth of millions of sequences per sample. P. Natl. Acad. Sci. U.S.A. 108, 4516–4522. https://doi.org/10.1073/pnas.1000080107.
- Chen, B.H., Wang, K., Dong, X., Lin, H., 2021. Long-term changes in red tide outbreaks in Xiamen Bay in China from 1986 to 2017. Estuar. Coast. Shelf Sci. 249 (107095) https://doi.org/10.1016/j.ecss.2020.107095.
- Dai, M.H., Yin, Z.Q., Meng, F.F., Liu, Q., Cai, W.J., 2012. Spatial distribution of riverine DOC inputs to the ocean: an updated global synthesis. Curr. Opin. Env. Sust. 4, 170–178. https://doi.org/10.1016/j.cosust.2012.03.003.
- Diaz, R.J., Rosenberg, R., Sturdivant, K., 2019. Hypoxia in estuaries and semi-enclosed seas, in Ocean Deoxygenation: Everyone's Problem - Causes, Impacts, Consequences and Solutions, eds D. Laffoley and J. M. Baxter (Gland: IUCN Global Marine and Polar Programme), 85–102.
- Dittmar, T., Koch, B., Hertkorn, N., Kattner, G., 2008. A simple and efficient method for the solid-phase extraction of dissolved organic matter (SPE-DOM) from seawater. Limnol. Oceanogr.-Meth. 6, 230–235. https://doi.org/10.4319/lom.2008.6.230.
- Fichot, C.G., Benner, R., 2014. The fate of terrigenous dissolved organic carbon in a river-influenced ocean margin. Global Biogeochem. Cy. 28, 300–318. https://doi.org/10.1002/2013gb004670.
- Flerus, R., Lechtenfeld, O.J., Koch, B.P., McCallister, S.L., Schmitt-Kopplin, P., Benner, R., Kaiser, K., Kattner, G., 2012. A molecular perspective on the ageing of marine dissolved organic matter. Biogeosciences. 9, 1935–1955. https://doi.org/ 10.5194/bg-9-1935-2012.
- Flores, G.E., Campbell, J.H., Kirshtein, J.D., Meneghin, J., Podar, M., Steinberg, J.I., Seewald, J.S., Tivey, M.K., Voytek, M.A., Yang, Z.K., Reysenbach, A.L., 2011. Microbial community structure of hydrothermal deposits from geochemically different vent fields along the Mid-Atlantic Ridge. Environ. Microbiol. 13, 2158–2171. https://doi.org/10.1111/j.1462-2920.2011.02463.x.
- Fox, B.G., Thorn, R.M.S., Anesio, A.M., Reynolds, D.M., 2017. The in situ bacterial production of fluorescent organic matter; an investigation at a species level. Water Res. 125. 350–359. https://doi.org/10.1016/j.watres.2017.08.040.
- Giovannoni, S.J., 2017. SAR11 bacteria: the most abundant plankton in the oceans. Ann. Rev. Mar. Sci. 9, 231–255. https://doi.org/10.1146/annurev-marine-010814-015934
- Gomez-Saez, G.V., Pohlabeln, A.M., Stubbins, A., Marsay, C.M., Dittmar, T., 2017.
  Photochemical alteration of dissolved organic sulfur from sulfidic porewater.
  Environ. Sci. Technol. 51, 14144–14154. https://doi.org/10.1021/acs.est.7b0371
- Gonsior, M., Luek, J., Schmitt-Kopplin, P., Grebmeier, J.M., Cooper, L.W., 2017. Optical properties and molecular diversity of dissolved organic matter in the Bering Strait and Chukchi Sea. Deep-Sea Res Pt Ii. 144, 104–111. https://doi.org/10.1016/j.dsr2.2017.01.003
- Gonsior, M., Zwartjes, M., Cooper, W.J., Song, W.H., Ishida, K.P., Tseng, L.Y., Jeung, M. K., Rosso, D., Hertkorn, N., Schmitt-Kopplin, P., 2011. Molecular characterization of effluent organic matter identified by ultrahigh resolution mass spectrometry. Water Res. 45, 2943–2953. https://doi.org/10.1016/j.watres.2011.03.016.
- Guo, W.D., Yang, L.Y., Hong, H.S., Stedmon, C.A., Wang, F.L., Xu, J., Xie, Y.Y., 2011. Assessing the dynamics of chromophoric dissolved organic matter in a subtropical estuary using parallel factor analysis. Mar. Chem. 124, 125–133. https://doi.org/ 10.1016/j.marchem.2011.01.003.
- Hansell, D.A., 2013. Recalcitrant dissolved organic carbon fractions. Ann. Rev. Mar. Sci. 5,421-445. https://doi.org/10.1146/annurev-marine-120710-100757.
- Hansell, D.A., Carlson, C.A., Schlitzer, R., 2012. Net removal of major marine dissolved organic carbon fractions in the subsurface ocean. Global Biogeochem. Cy. 26 https:// doi.org/10.1029/2011gb004069.
- He, C., Zhang, Y.H., Li, Y.Y., Zhuo, X.C., Li, Y.G., Zhang, C.L., Shi, Q., 2020a. In-house standard method for molecular characterization of dissolved organic matter by FT-ICR mass spectrometry. ACS Omega 5, 11730–11736. https://doi.org/10.1021/ acsomega.0c01055.
- He, C., Pan, Q., Li, P.H., Xie, W., He, D., Zhang, C.L., Shi, Q., 2020b. Molecular composition and spatial distribution of dissolved organic matter (DOM) in the Pearl River Estuary, China. Environ. Chem. 17, 240–251. https://doi.org/10.1071/En10051
- Herzsprung, P., Osterloh, K., von Tümpling, W., Harir, M., Hertkorn, N., Schmitt-Kopplin, P., Meissner, R., Bernsdorf, S., Friese, K., 2017. Differences in DOM of rewetted and natural peatlands—Results from high-field FT-ICR-MS and bulk optical parameters. Sci. Total Environ. 586, 770–781. https://doi.org/10.1016/j.scitotenv.2017.02.054.
- Herzsprung, P., von Tümpling, W., Hertkorn, N., Harir, M., Büttner, O., Bravidor, J., Friese, K., Schmitt-Kopplin, P., 2012. Variations of DOM quality in inflows of a drinking water reservoir: linking of van Krevelen diagrams with EEMF spectra by rank correlation. Environ. Sci. Technol. 46,5511-5518. https://doi.org/10.1021/ es300345c.
- Hewson, I., Fuhrman, J.A., 2004. Richness and diversity of bacterioplankton species along an estuarine gradient in Moreton Bay, Australia. Appl. Environ. Microb. 70, 3425–3433. https://doi.org/10.1128/Aem.70.6.3425-3433.2004.
- Ibarbalz, F.M., Henry, N., Brandao, M.C., Martini, V., Busseni, G., Byrne, H., Coelho, L.P., Endo, H., Gasol, J.M., Gregory, A.C., Mahe, F., Rigonato, J., Royo-Llonch, M., Salazar, G., Sanz-Saez, I., Scalco, E., Soviadan, D., Zayed, A.A., Zingone, A., Labadie, K., Ferland, J., Marec, C., Kandels, S., Picheral, M., Dimier, C., Poulain, J., Pisarev,

- S., Carmichael, M., Pesant, S., Acinas, S.G., Babin, M., Bork, P., Boss, E., Bowler, C., Cochrane, G., de Vargas, C., Follows, M., Gorsky, G., Grimsley, N., Guidi, L., Hingamp, P., Iudicone, D., Jaillon, O., Kandels, S., Karp-Boss, L., Karsenti, E., Not, F., Ogata, H., Pesant, S., Poulton, N., Raes, J., Sardet, C., Speich, S., Stemmann, L., Sullivan, M.B., Sunagawa, S., Wincker, P., Bopp, L., Lombard, F., Zinger, L., Coordinators, T.O., 2019. Global trends in marine plankton diversity across kingdoms of life. Cell. 179,1084-+. https://doi.org/10.1016/j.cell.2019.10.008.
- Jiao, N., Herndl, G.J., Hansell, D.A., Benner, R., Kattner, G., Wilhelm, S.W., Kirchman, D. L., Weinbauer, M.G., Luo, T.W., Chen, F., Azam, F., 2010. Microbial production of recalcitrant dissolved organic matter: long-term carbon storage in the global ocean. Nat. Rev. Microbiol. 8, 593–599. https://doi.org/10.1038/nrmicro2386.
- Jiao, N., Robinson, C., Azam, F., Thomas, H., Baltar, F., Dang, H., Hardman-Mountford, N.J., Johnson, M., Kirchman, D.L., Koch, B.P., Legendre, L., Li, C., Liu, J., Luo, T., Luo, Y.W., Mitra, A., Romanou, A., Tang, K., Wang, X., Zhang, C., Zhang, R., 2014. Mechanisms of microbial carbon sequestration in the ocean future research directions. Biogeosciences 11, 5285–5306. https://doi.org/10.5194/bg-11-5285-2014
- Kamjunke, N., Nimptsch, J., Harir, M., Herzsprung, P., Schmitt-Kopplin, P., Neu, T.R., Graeber, D., Osorio, S., Valenzuela, J., Reyes, J.C., Woelfl, S., Hertkorn, N., 2017. Land-based salmon aquacultures change the quality and bacterial degradation of riverine dissolved organic matter. Sci. Rep.-Uk. 7, 1–15. https://doi.org/10.1038/ srep43739.
- Knap, A., Michaels, A., Close, A., Ducklow, H., Dickson, A., 1996. Protocols for the joint global ocean flux study (JGOFS) core measurements. https://doi.org/10.1007/ bf02986941
- Koch, B.P., Dittmar, T., 2006. From mass to structure: an aromaticity index for high-resolution mass data of natural organic matter. Rapid Commun. Mass Spectrom. 20, 926–932. https://doi.org/10.1002/rcm.2386.
- Koch, B.P., Witt, M.R., Engbrodt, R., Dittmar, T., Kattner, G., 2005. Molecular formulae of marine and terrigenous dissolved organic matter detected by electrospray ionization Fourier transform ion cyclotron resonance mass spectrometry. Geochim. Cosmochim. Ac. 69, 3299–3308. https://doi.org/10.1016/j.gca.2005.02.027.
- Krogh, J., Ianson, D., Hamme, R.C., Lowe, C.J., 2018. Risks of hypoxia and acidification in the high energy coastal environment near Victoria, Canada's untreated municipal sewage outfalls. Mar. Pollut. Bull. 133, 517–531. https://doi.org/10.1016/j. marpolbul.2018.05.018.
- Ksionzek, K.B., Lechtenfeld, O.J., McCallister, S.L., Schmitt-Kopplin, P., Geuer, J.K., Geibert, W., Koch, B.P., 2016. Dissolved organic sulfur in the ocean: Biogeochemistry of a petagram inventory. Science 354, 456–459. https://doi.org/ 10.1126/science.aaf7796.
- Kujawinski, E.B., 2011. The impact of microbial metabolism on marine dissolved organic matter. Ann. Rev. Mar. Sci. 3, 567–599. https://doi.org/10.1146/annurev-marine-120308-081003.
- Landa, M., Cottrell, M.T., Kirchman, D.L., Kaiser, K., Medeiros, P.M., Tremblay, L., Batailler, N., Caparros, J., Catala, P., Escoubeyrou, K., Oriol, L., Blain, S., Obernosterer, I., 2014. Phylogenetic and structural response of heterotrophic bacteria to dissolved organic matter of different chemical composition in a continuous culture study. Environ. Microbiol. 16, 1668–1681. https://doi.org/10.1111/1462-2920.12242.
- Lechtenfeld, O.J., Kattner, G., Flerus, R., McCallister, S.L., Schmitt-Kopplin, P., Koch, B. P., 2014. Molecular transformation and degradation of refractory dissolved organic matter in the Atlantic and Southern Ocean. Geochim. Cosmochim. Acta 126, 321–337. https://doi.org/10.1016/j.gca.2013.11.009.
- Lønborg, C., Middelboe, M., Brussaard, C.P., 2013. Viral lysis of Micromonas pusilla: impacts on dissolved organic matter production and composition. Biogeochemistry 116, 231–240. https://doi.org/10.1007/s10533-013-9853-1.
- Lønborg, C., Carreira, C., Jickells, T., Ivarez-Salgado, X.-A., 2020. Impacts of global change on ocean dissolved organic carbon (DOC) cycling. Frontiers in Mar. Sci. 7,466-. https://doi.org/10.3389/fmars.2020.00466.
- Ludwig, W., Probst, J.L., Kempe, S., 1996. Predicting the oceanic input of organic carbon by continental erosion. Global Biogeochem. Cy. 10, 23–41. https://doi.org/10.1029/ 95gb02925.
- Luo, H.W., Cusros, M., Hughes, A.L., Moran, M.A., 2013. Evolution of divergent life history strategies in marine alphaproteobacteria. Mbio 4. https://doi.org/10.1128/ pbio.00373.13
- Mentges, A., Feenders, C., Seibt, M., Blasius, B., Dittmar, T., 2017. Functional molecular diversity of marine dissolved organic matter is reduced during degradation. Front. Mar. Sci. 4, 194. https://doi.org/10.3389/fmars.2017.00194.
- Miranda, M.L., Osterholz, H., Giebel, H.-A., Bruhnke, P., Dittmar, T., Zielinski, O., 2020. Impact of UV radiation on DOM transformation on molecular level using FT-ICR-MS and PARAFAC. Spectrochim. Acta Part A: Mol. Biomol. Spectroscopy 230, 118027. https://doi.org/10.3389/fmars.2017.00194.
- Murphy, K.R., Stedmon, C.A., Graeber, D., Bro, R., 2013. Fluorescence spectroscopy and multi-way techniques. PARAFAC. Anal. Methods-Uk. 5, 6557–6566. https://doi.org/ 10.1039/c3av41160e.
- Osterholz, H., Kirchman, D.L., Niggemann, J., Dittmar, T., 2018. Diversity of bacterial communities and dissolved organic matter in a temperate estuary. FEMS Microbiol. Ecol. 94, fiy119. https://doi.org/10.1093/femsec/fiy119.
- Osterholz, H., Niggemann, J., Giebel, H.A., Simon, M., Dittmar, T., 2015. Inefficient microbial production of refractory dissolved organic matter in the ocean. Nat. Commun. 6, 1–8. https://doi.org/10.1038/ncomms8422.
- Osterholz, H., Singer, G., Wemheuer, B., Daniel, R., Simon, M., Niggemann, J., Dittmar, T., 2016. Deciphering associations between dissolved organic molecules and bacterial communities in a pelagic marine system. ISME J. 10, 1717–1730. https://doi.org/10.1038/ismej.2015.231.

- Patriarca, C., Sedano-Núñez, V.T., Garcia, S.L., Bergquist, J., Bertilsson, S., Sjöberg, P.J., Tranvik, L.J., Hawkes, J.A., 2020. Character and environmental lability of cyanobacteria-derived dissolved organic matter. Limnology Oceanography. https:// doi.org/doi.org/10.1002/lno.11619.
- Pohlabeln, A.M., Gomez-Saez, G.V., Noriega-Ortega, B.E., Dittmar, T., 2017. Experimental evidence for abiotic sulfurization of marine dissolved organic matter. Front. Mar. Sci. 4, 364. https://doi.org/10.3389/fmars.2017.00364.
- Powers, L.C., Luek, J.L., Schmitt-Kopplin, P., Campbell, B.J., Magen, C., Cooper, L.W., Gonsior, M., 2018. Seasonal changes in dissolved organic matter composition in Delaware Bay, USA in March and August 2014. Org Geochem. 122, 87–97. https://doi.org/10.1016/j.orggeochem.2018.05.005.
- Romera-Castillo, C., Sarmento, H., Alvarez-Salgado, X.A., Gasol, J.M., Marrasé, C., 2011. Net production and consumption of fluorescent colored dissolved organic matter by natural bacterial assemblages growing on marine phytoplankton exudates. Appl. Environ. Microbiol. 77, 7490–7498. https://doi.org/10.1128/AEM.00200-11.
- Schmidt, F., Elvert, M., Koch, B.P., Witt, M., Hinrichs, K.U., 2009. Molecular characterization of dissolved organic matter in pore water of continental shelf sediments. Geochim. Cosmochim. Ac. 73, 3337–3358. https://doi.org/10.1016/j. gca.2009.03.008.
- Seidel, M., Dittmar, T., Ward, N.D., Krusche, A.V., Richey, J.E., Yager, P.L., Medeiros, P. M., 2016. Seasonal and spatial variability of dissolved organic matter composition in the lower Amazon River. Biogeochemistry 131, 281–302. https://doi.org/10.1007/s10533.016.0279.4
- Seidel, M., Yager, P.L., Ward, N.D., Carpenter, E.J., Gomes, H.R., Krusche, A.V., Richey, J.E., Dittmar, T., Medeiros, P.M., 2015. Molecular-level changes of dissolved organic matter along the Amazon River-to-ocean continuum. Mar. Chem. 177, 218–231. https://doi.org/10.1016/j.marchem.2015.06.019.
- Sheik, C.S., Cleaves, H.J., Johnson-Finn, K., Giovannelli, D., Kieft, T.L., Papineau, D., Schrenk, M.O., Tumiati, S., 2020. Abiotic and biotic processes that drive carboxylation and decarboxylation reactions. Am. Mineral. 105, 609–615. https://doi.org/10.2138/am-2020-7166CCBYNCND.
- Stedmon, C.A., Seredynska-Sobecka, B., Boe-Hansen, R., Le Tallec, N., Waul, C.K., Arvin, E., 2011. A potential approach for monitoring drinking water quality from groundwater systems using organic matter fluorescence as an early warning for contamination events. Water Res. 45, 6030–6038. https://doi.org/10.1016/j. watres.2011.08.066.
- Stubbins, A., Lapierre, J.F., Berggren, M., Prairie, Y.T., Dittmar, T., del Giorgio, P.A., 2014. What's in an EEM? Molecular signatures associated with dissolved organic fluorescence in Boreal Canada. Environ. Sci. Technol. 48, 10598–10606. https://doi. org/10.1021/es502086e.
- Tanentzap, A.J., Fitch, A., Orland, C., Emilson, E.J.S., Yakimovich, K.M., Osterholz, H., Dittmar, T., 2019. Chemical and microbial diversity covary in fresh water to influence ecosystem functioning. Proc. Natl. Acad. Sci. U. S. A. 116, 24689–24695. https://doi.org/10.1073/pnas.1904896116.
- Teeling, H., Fuchs, B.M., Becher, D., Klockow, C., Gardebrecht, A., Bennke, C.M., Kassabgy, M., Huang, S.X., Mann, A.J., Waldmann, J., Weber, M., Klindworth, A., Otto, A., Lange, J., Bernhardt, J., Reinsch, C., Hecker, M., Peplies, J., Bockelmann, F. D., Callies, U., Gerdts, G., Wichels, A., Wiltshire, K.H., Glockner, F.O., Schweder, T., Amann, R., 2012. Substrate-controlled succession of marine bacterioplankton populations induced by a phytoplankton bloom. Science 336, 608–611. https://doi.org/10.1126/science.1218344.
- Traving, S.J., Rowe, O., Jakobsen, N.M., Sorensen, H., Dinasquet, J., Stedmon, C.A., Andersson, A., Riemann, L., 2017. The effect of increased loads of dissolved organic matter on estuarine microbial community composition and function. Front. Microbiol. 8, 351. https://doi.org/10.3389/fmicb.2017.00351.
- Vorobev, A., Sharma, S., Yu, M.Y., Lee, J., Washington, B.J., Whitman, W.B., Ballantyne, F., Medeiros, P.M., Moran, M.A., 2018. Identifying labile DOM components in a coastal ocean through depleted bacterial transcripts and chemical signals. Environ. Microbiol. 20, 3012–3030. https://doi.org/10.1111/1462-2920.14344.
- Wang, Y., Liu, Y.T., Wang, J.N., Luo, T.W., Zhang, R., Sun, J., Zheng, Q., Jiao, N.Z., 2019. Seasonal dynamics of bacterial communities in the surface seawater around subtropical Xiamen Island, China, as determined by 16S rRNA gene profiling. Mar. Pollut. Bull. 142, 135–144. https://doi.org/10.1016/j.marpolbul.2019.03.035.
- Wang, Y., Zhang, R., He, Z.L., Van Nostrand, J.D., Zheng, Q., Zhou, J.Z., Jiao, N.Z., 2017. Functional gene diversity and metabolic potential of the microbial community in an estuary-shelf environment. Front. Microbiol. 8, 1153. https://doi.org/10.3389/ fmicb.2017.01153.
- Watson, A.J., Lenton, T.M., Mills, B.J.W., 2017. Ocean deoxygenation, the global phosphorus cycle and the possibility of human-caused large-scale ocean anoxia. Philos. Trans. A Math. Phys. Eng. Sci. 375, 20160318-. https://doi.org/10.1098/ rsta.2016.0318
- Wemheuer, B., Wemheuer, F., Daniel, R., 2012. RNA-based assessment of diversity and composition of active archaeal communities in the German bight. Archaea 2012. https://doi.org/10.1155/2012/695826.
- Wetzel, R.G., Hatcher, P.G., Bianchi, T.S., 1995. Natural photolysis by ultraviolet irradiance of recalcitrant dissolved organic matter to simple substrates for rapidbacterial metabolism. Limnol. Oceanogr. 40, 1369–1380. https://doi.org/ 10.4319/lo.1995.40.8.1369.
- Whitman, W.B., Coleman, D.C., Wiebe, W.J., 1998. Prokaryotes: The unseen majority.
  P. Natl. Acad. Sci. U.S.A. 95, 6578–6583. https://doi.org/10.1073/pnas.95.12.6578.
- Yan, X.L., Zhai, W.D., Hong, H.S., Li, Y., Guo, W.D., Huang, X., 2012. Distribution, fluxes and decadal changes of nutrients in the Jiulong River Estuary, Southwest Taiwan Strait. Chin. Sci. Bull. 57, 2307–2318. https://doi.org/10.1007/s11434-012-5084-4.

- Yang, C., Li, Y., Zhou, Y., Zheng, W., Tian, Y., Zheng, T., 2012. Bacterial community dynamics during a bloom caused by Akashiwo sanguinea in the Xiamen sea area.
- China. Harmful algae. 20, 132–141. https://doi.org/10.1016/j.hal.2012.09.002.

  Yang, C.Y., Li, Y., Zhou, B., Zhou, Y.Y., Zheng, W., Tian, Y., Van Nostrand, J.D., Wu, L.Y., He, Z.L., Zhou, J.Z., Zheng, T.L., 2015. Illumina sequencing-based analysis of free-living bacterial community dynamics during an Akashiwo sanguine bloom in Xiamen sea. China. Sci. Rep.-Uk. 5, 8476. https://doi.org/10.1038/srep08476.
- Zhao, Z., Gonsior, M., Schmitt-Kopplin, P., Zhan, Y.C., Zhang, R., Jiao, N.Z., Chen, F., 2019. Microbial transformation of virus-induced dissolved organic matter from picocyanobacteria: coupling of bacterial diversity and DOM chemodiversity. ISME J. 13, 2551–2565. https://doi.org/10.1038/s41396-019-0449-1.
- Zheng, Q., Chen, Q., Cai, R., He, C., Guo, W., Wang, Y., Shi, Q., Chen, C., Jiao, N., 2019. Molecular characteristics of microbially mediated transformations of Synechococcus-derived dissolved organic matter as revealed by incubation experiments. Environ. Microbiol. 21, 2533–2543. https://doi.org/10.1111/1462-2920.14646.
- Zheng, Q., Wang, Y., Xie, R., Lang, A.S., Liu, Y.T., Lu, J.Y., Zhang, X.D., Sun, J., Suttle, C. A., Jiao, N.Z., 2018. Dynamics of heterotrophic bacterial assemblages within synechococcus cultures. Appl. Environ. Microb. 84 https://doi.org/10.1128/AEM.01517-17.